European Journal of Medicinal Chemistry 48 (2012) 206–213

Contents lists available at SciVerse ScienceDirect

European Journal of Medicinal Chemistry

journal homepage: http://www.elsevier.com/locate/ejmech

Original article

A small chemical library of 2-aminoimidazole derivatives as BACE-1 inhibitors: Structure-based design, synthesis, and biological evaluation

Gianpaolo Chiriano [a,b], Angela De Simone [c], Francesca Mancini [c], Daniel I. Perez [d], Andrea Cavalli [c,e], Maria Laura Bolognesi [c], Giuseppe Legname [f], Ana Martinez [d], Vincenza Andrisano [c], Paolo Carloni [g], Marinella Roberti [c,*]

[a] Statistical and Biological Physics Sector, SISSA-ISAS, Via Bonomea 265, 34136 Trieste, Italy
[b] Italian Institute of Technology, SISSA-ISAS Unit, Italy
[c] Department of Pharmaceutical Sciences, University of Bologna, Via Belmeloro 6, 40126 Bologna, Italy
[d] Instituto de Quimica Medica-CSIC, Juan de la Cierva 3, 28006 Madrid, Spain
[e] Department of Drug Discovery and Development, Italian Institute of Technology, Via Morego 30, 16163 Genova, Italy
[f] Neurobiology Sector, SISSA-ISAS, Via Bonomea 265, 34136 Trieste, Italy
[g] German Research School for Simulation Sciences GmbH, 52425 Jülich, Germany

ARTICLE INFO

Article history:
Received 23 June 2011
Received in revised form
3 November 2011
Accepted 9 December 2011
Available online 16 December 2011

Keywords:
Alzheimer's disease
Amyloid-beta peptide
Drug design
Hit identification
2-Aminoimidazole

ABSTRACT

In this work, we report a rational structure-based approach aimed at the discovery of new 2-aminoimidazoles as β-secretase inhibitors. Taking advantage of a microwave-assisted synthetic protocol, a small library of derivatives was obtained and biologically evaluated. Two compounds showed promising activities in both enzymatic and cellular assays. Moreover, one of them exhibited the capability to cross the blood–brain barrier as assessed by the parallel artificial membrane permeability assay.

1. Introduction

Alzheimer's disease (AD) is a progressive and fatal brain disorder, for which there is no cure. AD causes memory loss, steady deterioration of cognition, and dementia afflicting currently over 30 million people worldwide. By 2050, estimates range as high as more than 100 million Alzheimer's patients worldwide (World Alzheimer Report 2010) (http://www.alz.org/). One of the major characteristic and pathological hallmarks of AD is represented by the senile plaques, whose main component is the amyloid-β peptide (Aβ) [1].

Aβ forms toxic extra-cellular (proto)-fibrils, which initiate the pathogenic cascade [2]. Thus, the discovery of compounds able to modulate the production and clearance of Aβ represents a key strategy in the field of AD [3–5]. Aβ is generated by sequential proteolytic cleavage of a large trans-membrane protein, the amyloid precursor protein (APP), by two proteases, β- and γ-secretase. Therefore, β- and γ-secretase enzymes have been studied in depth in the search for inhibitors as potential anti-AD drugs. In this scenario, while a β-secretase inhibitor, CTS-21666 from CoMentis, advanced up to Phase II clinical trials [6], a γ-secretase inhibitor failed in Phase III clinical trials because of lack of efficacy and increased risk of skin cancer [7]. Furthermore, the presence of several structural information related to β-secretase makes it a very suitable target for structure-based drug design purposes [8].

The first β-secretase inhibitors were peptide and peptidomimetic compounds successfully designed as transition state analogs showing a nanomolar affinity for β-secretase [9,10]. The crystal structures of these inhibitors in complex with the enzyme have been utilized for structure-based projects that have led to the

Abbreviations: AD, Alzheimer's Disease; Aβ, amyloid-β peptide; APP, amyloid precursor protein; BBB, blood–brain barrier; BACE-1, β-secretase APP cleaving enzyme; cLogP, calculated decimal logarithm of octanol/water partition coefficient; CNS, central nervous system; ESP, electrostatic potential; HTS, high-throughput screening; PAMPA, parallel artificial membrane permeability assay; TPSA, topological polar surface area.

* Corresponding author. Fax: +39 051 2099734.
E-mail address: marinella.roberti@unibo.it (M. Roberti).

0223-5234/$ – see front matter © 2011 Elsevier Masson SAS. All rights reserved.
doi:10.1016/j.ejmech.2011.12.016

discovery of several classes of compounds with improved pharmacokinetics properties [11]. In particular, there was a boom in the development of non-peptidic β-secretase inhibitors that have been discovered by means of different approaches, such as high-throughput screening (HTS), fragment-based, and structure-based strategies [12–14]. Compared with traditional HTS, a significantly higher *hit* rate can be obtained by using a structure-based approach, which can fully exploit the large amount of structural information related to β-secretase.

In this paper, we report on the structure-based design and microwave-assisted synthesis of a novel small library of 2-aminoimidazoles as β-secretase inhibitors.

2. Design

The β-secretase APP cleaving enzyme (BACE-1) is a member of the pepsin-like family of aspartyl proteases. It is a class I transmembrane protein characterized by an NH_2-terminal protease domain structurally well-defined, a connecting strand, a transmembrane region, and a cytosolic domain [15].

Initially, we aimed at identifying a moiety potentially interacting with the catalytic aspartic dyad of the enzyme. In particular, among the possible scaffolds, the 2-aminoimidazole appeared to be a very attractive moiety for the following reasons: i) it contains the guanidinium function, which can provide optimal interactions with the catalytic aspartic dyad (see Supporting Information (SI)), as also demonstrated by the crystal structures of several guanidinium-carrying inhibitors in complex with BACE-1 [12]; ii) it is a privileged structure [16]; iii) it allows the parallel synthesis of differently polysubstituted derivatives [17,18]. Therefore, the 2-aminoimidazole was docked to validate its capability to interact with the catalytic dyad of BACE-1. As expected, the 2-aminoimidazole turned out to be oriented in the center of the rather large BACE-1 binding pocket by interacting with both catalytic aspartic acids, Asp32 and Asp228, via electrostatic and H-bond interactions (see SI). Then, among the 2-aminoimidazoles reported in the literature [16,18,19], the fragment **1** [18] shown in Fig. 1 turned out to be particularly well-suited for drug discovery purposes for the following reasons: **1** has a low molecular weight (MW = 263.34) and displays a rather good chemical accessibility, which could allow for generating library of compounds. This fragment was preliminary investigated by means of docking simulations. The binding mode of **1** at BACE-1 binding pocket is reported in Fig. 1. The following interactions were identified: i) the guanidinium moiety of **1** interacted with both aspartic acids (Asp32 and Asp228) side chains and with Thr232; ii) one of the two phenyl rings formed hydrophobic interactions (with Val69, Trp76, Phe108) and a π–π stacking with Tyr71; iii) the second phenyl ring established a cation-π interaction with the side chain of Arg235.

In light of this computational result, **1** was tested against BACE-1 using an enzymatic assay [20]. It exhibited a moderate-to-low inhibitor potency at 100 μM concentration (BACE-1 inhibition % = 19.64 ± 0.69). On these bases, decorating fragment **1**, we designed and synthesized a small library of 2-aminoimidazoles.

3. Chemistry

The 2-aminoimidazoles, **1**–**11**, were obtained taking advantage of a microwave-assisted, one-pot, two-step protocol [18] based on the cyclocondensation of 2-benzylaminopyrimidines **12a**–**d** and appropriate 3-substituted-α-bromopropyl aldehydes **13a**–**f**, followed by the cleavage of the corresponding not isolated intermediate imidazo[1,2-*a*]pyrimidin-1-ium salts with an excess of hydrazine (Scheme 1). The 2-benzylaminopyrimidines **12a**–**d** were synthesized in parallel by reaction of commercially available benzylbromides **14a**–**d** with excess of 2-aminopyrimidine **15** and sodium hydride (Scheme 2). The α-bromo aldehydes **13a**–**f** were obtained in a parallel fashion using the following synthetic pathway. A cross-coupling Suzuki reaction between the 3-(bromophenyl)-propionic methyl esters **16**,**17**, which can be easily accessed from the corresponding 3-(bromophenyl)-propanoic acids, and the appropriate boronic acids **18**–**21** in the presence of a catalytic amount of tetrakis (triphenylphosphine) palladium $Pd(PPh_3)_4$ gave the 3-biphenyl propanoic methyl esters **22a**–**e**, respectively. These were reduced to the corresponding 3-biphenyl propyl alcohols **23a**–**e**. Oxidation of **23a**–**e** and commercially available 3-phenylpropanol **23f** gave the corresponding 3-substituted propyl aldehydes **24a**–**f**, which were brominated in mild conditions using 0.5 equivalent of 5,5-dibromobarbituric acid (DBBA) to provide the required 3-substituted-α-bromopropyl aldehydes **13a**–**f** (Scheme 3).

4. Biology

2–**11** were first tested in biochemical assays performed using the fluorescence resonance energy transfer (FRET) methodology [20]. The BACE-1 inhibition studies were based on the cleavage of peptide substrate mimicking the human APP sequence with the Swedish mutation (Methoxycoumarin-Ser-Glu-Val-Asn-Leu-Asp-Ala-Glu-Phe-Lys-dinitrophenyl, M-2420, Bachem, Germany) [20] (see SI). **2**–**11** were tested at a concentration of 5 μM and their BACE-1 inhibition percentages are reported in Table 1. The IC_{50} values of most active compounds (**7**–**9** and **11**) were determined by using the linear regression parameters. Subsequently, the capability of **7**–**9**

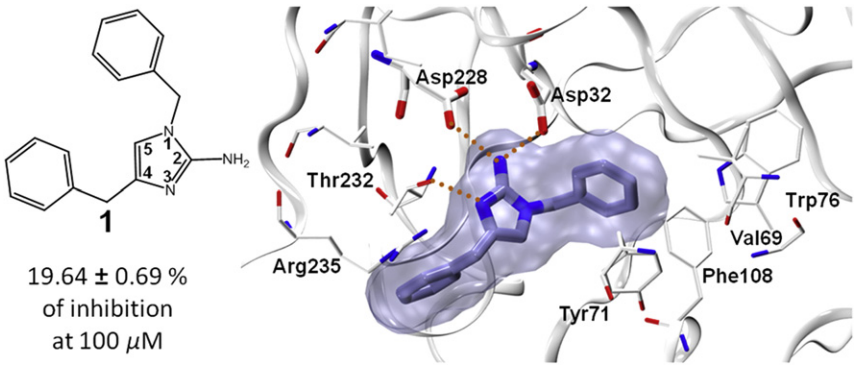

Fig. 1. Low-energy docking model of the BACE-1/1 complex and the main interactions are highlighted by orange points. (For interpretation of the references to colour in this figure legend, the reader is referred to the web version of this article.)

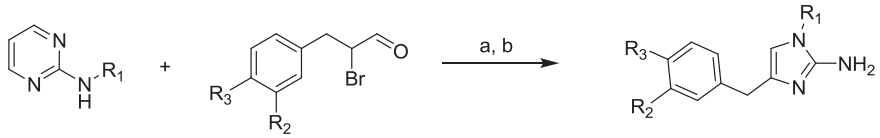

12a: R_1=Bn
12b: R_1=4-FBn
12c: R_1=3,5-FBn
12d: R_1=2-ClBn

13a: R_2=3,5-diOMePh; R_3=H
13b: R_2=H; R_3=3,5-diOMePh
13c: R_2=H; R_3=4-CF_3Ph
13d: R_2=H; R_3=3-benzyloxyPh
13e: R_2=H; R_3=4-(dibenzo[*b*,*d*] furan-1-yl)
13f: R_2=R_3=H

1: R_1=Bn; R_2=H; R_3=H
2: R_1=4-FBn; R_2=H; R_3=H
3: R_1=3,5-diFBn; R_2=H; R_3=H
4: R_1=2-ClBn; R_2=H; R_3=H
5: R_1=4-FBn; R_2=3,5-diOMePh; R_3=H
6: R_1=3,5-diFBn; R_2=3,5-diOMePh; R_3=H
7: R_1=4-FBn; R_2=H; R_3=3,5-diOMePh
8: R_1=3,5-diFBn; R_2=H; R_3=3,5-diOMePh
9: R_1=3,5-diFBn; R_2=H; R_3=4-CF_3Ph
10: R_1=3,5-diFBn; R_2=H; R_3=3-benzyloxyPh
11: R_1=2-ClBn; R_2=H; R_3=4-(dibenzo[*b*,*d*] furan-1-yl)

Scheme 1. Reagents and conditions: a) MeCN, 150 °C, 150 W; b) 60% hydrazine (5 equiv), MeCN, 100 °C, 100 W.

and **11** to modulate APP processing was examined by performing a cell-based ELISA assay. This study was carried out in primary chicken telencephalon neurons to assess the effect of the most active inhibitors on secretion of Aβ$_{38}$, Aβ$_{40}$ and Aβ$_{42}$ [21] (see SI).

5. Results and discussion

As previously described, our strategy was based on **1** as the starting fragment for generating a new series of BACE-1 inhibitors. In particular, we attempted to improve the low potency of **1** (see Fig. 1) by initially modifying the electronic and hydrophobic properties of the benzyl group in position R_1 (see Scheme 1) through the introduction of fluorine and chlorine atoms in different positions (see compounds **2**–**4** in Table 1). These substitutions allowed **2**–**4** to consolidate the hydrophobic interactions observed for **1** (Fig. 1) and to potentially establish H-bonds (for the fluorine derivatives) with the OH of Tyr71 and NH of Trp76 side chains. As expected, **2**–**4** showed a BACE-1 inhibitory potency notably increased when compared to that of **1** (see Table 1). To inspect for possible correlations between electronic properties and BACE-1 inhibition, the electrostatic potential (ESP) surfaces were calculated for **2**–**4**. A qualitative relationship was observed between an increased inhibition percentage and a decreased negative character of the aromatic ring in R_1 (see Fig. S4 in SI). In particular, when compared to **1**, **2**–**4** appeared to have an electron-poorer benzyl group (R_1) that could allow this moiety to establish more favorable π–π stacking with electron-rich aromatic residues located in the binding pocket (i.e. Tyr71 and Trp76). In addition, from a pharmacokinetic perspective, the presence of fluorine atoms on an aromatic ring could improve the metabolic stability, by avoiding a probable aromatic hydroxylation mechanism [22].

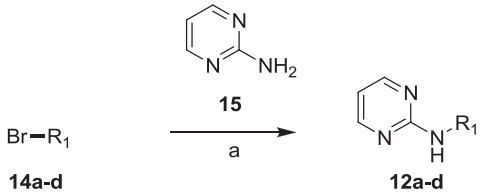

14a: R_1=Bn
14b: R_1=4-FBn
14c: R_1=3,5-diFBn
14d: R_1=2-ClBn

12a: R_1=Bn
12b: R_1=4-FBn
12c: R_1=3,5-diFBn
12d: R_1=2-ClBn

Scheme 2. Reagents and conditions: a) NaH, THF, 24 h, room temperature.

To increase the chemical diversity, we then synthesized a second series of derivatives, **5**–**11**, maintaining a halogenated benzyl group in R_1 and bearing differently substituted aromatic rings in R_2 and R_3 (*meta* and *para* positions, see Scheme 1). All compounds showed a BACE-1 inhibitory profile. In particular, **7**–**9** and **11** showed IC_{50} values in the low micromolar range (see Table 1). To characterize the binding mode of one of the most active inhibitors, docking and molecular dynamics (MD) simulations were carried out using BACE-1 (PDB ID: 1SGZ) [23] and **7** (see Fig. 2 and SI). The following interactions were observed for the best-ranked pose as obtained using the Goldscore scoring function (see SI): i) the amino group (NH_2) of **7** interacts via H-bond with the catalytic dyad; ii) the N3 nitrogen of the imidazole ring establishes electrostatic and H-bond interactions with the side chains of Asp228 and Thr232, respectively; iii) the fluorine atom interacts with the NH of Trp76 side chain; iv) the benzyl ring establishes favorable π–π stacking with the side chain of Tyr71 and hydrophobic interactions with Val69, Trp76, and Phe108; v) the phenyl group mounted on the C4 of the imidazole ring interacts via cation-π with the Arg235; vi) the polymethoxylated substituent in R_3 might establish H-bond interactions with the side chains of Asn233 and Lys321, both residues located in a solvent-exposed region of the active site. Notably, once this complex was already computationally generated, the X-ray structure of a 2-aminoimidazole derivative in complex with BACE-1 was published by researchers from Merck [24,25]. Interestingly enough, our predicted binding mode was remarkably similar to that reported [24,25] showing as pivotal interactions the salt-bridge between the guanidinium moiety and the aspartic dyad. To further investigate the role of these electrostatic interactions, we monitored the stability of these salt bridges throughout 100 ns of MD simulations (see SI for further details). Both interactions were remarkably stable showing that the guanidinium was the anchoring point of our inhibitors at BACE-1 active site.

In light of these results, **7**–**9** and **11** were tested using cellular assays based on the secretion of Aβ$_{38}$, Aβ$_{40}$ and Aβ$_{42}$ and on cell viability in primary chicken telencephalon neurons [21]. The IC_{50} values reported in Table 2 have been corrected with mean neurons viability obtained in the MTT reduction assay (see SI). **7** was the most active compound inhibiting Aβ$_{38}$, Aβ$_{40}$, and Aβ$_{42}$ secretion with IC_{50} values of 15, 23 and 19 μM respectively, and starting to be moderately toxic at 25 μM. Otherwise, **8** started to display toxic effects at 50 μM, and reduced Aβ$_{38}$, Aβ$_{40}$, and Aβ$_{42}$ secretion with higher IC_{50} values than **7** (33, 35 and 27 μM respectively). In contrast, **9** and **11** resulted inactive. To explain the different activity of derivatives **7**–**9** and **11** in cellular assays, we explored some of

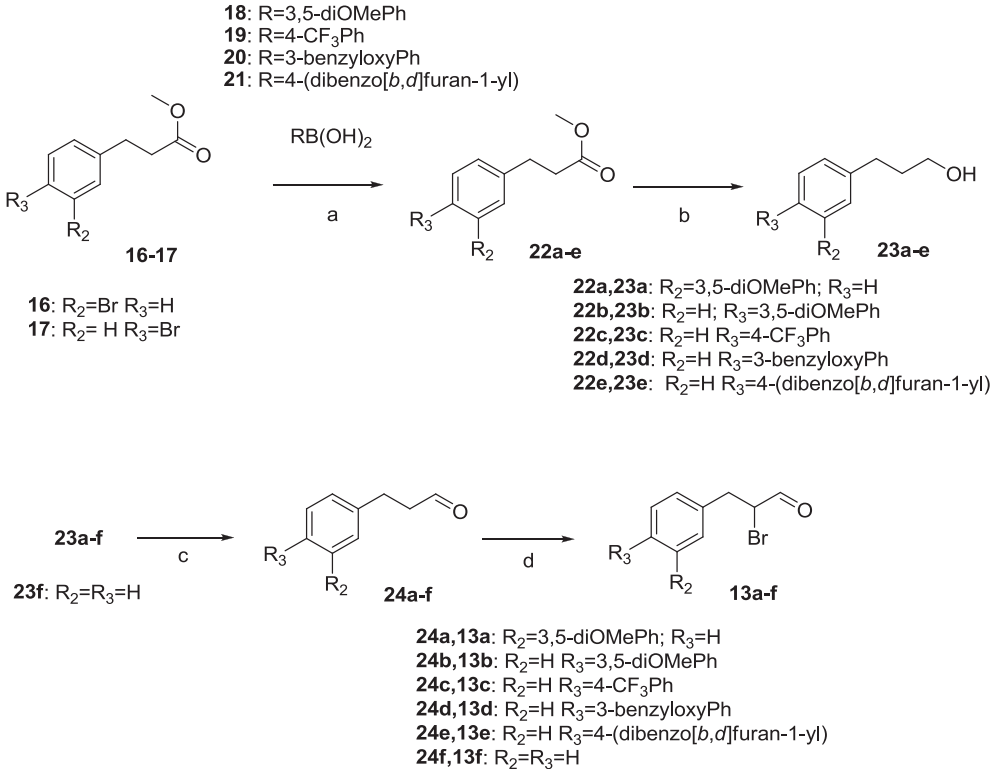

Scheme 3. Reagents and conditions: a) $Pd(PPh_3)_4$, Na_2CO_3 (aq), toluene:EtOH (2:1), 5 h, reflux; b) $LiAlH_4$, Et_2O, 0 °C, 5 h; c) PCC (1.4 equiv), CH_2Cl_2, 0 °C, 3 h; d) DBBA (0.5 equiv), Et_2O, HCl (cat).

their molecular descriptors such as calculated decimal logarithm of octanol/water partition coefficient (cLogP) and topological polar surface area (TPSA). **9** and **11** showed higher cLogP and lower TPSA values when compared to **7** and **8** (see Table 2). Finally, since an anti-AD drug candidate must work at central nervous system (CNS) level, we studied the capability of **7**–**9** and **11** to cross the blood–brain barrier (BBB) by using the parallel artificial membrane permeability assay (PAMPA), as described by Di et al. [26] (see SI). As shown by the *in vitro* permeability (*Pe*) values (Table 2), **8** BBB permeation was predicted to be low, **9** was not examined because of its insolubility in the experimental conditions here employed, whereas **7** and **11** were predicted to be able to cross the BBB by passive permeation. Moreover, the calculated LogP and TPSA values of **7** and **8** in their protonated form are in agreement with the optimal physical–chemical parameters for targeting CNS drugs [27,28]. Differently, the cLogP values are to high both for **9** and **11**, whereas the TPSA value is low for **9** and proper for **11** (see Table 2).

In light of this series of experiments, it turned out that **7** was a promising *hit* to undergo to a subsequent *hit*-to-*lead* campaign. Interestingly, structurally similar compounds recently reported by Hills et al. [25] have shown relatively low Pgp efflux, pointing to this class of molecules as promising BACE-1 *lead* candidates. Indeed, our result could be particularly hopeful in the context of the 2-aminoimidazole-based BACE-1 inhibitors, where a major issue is the BBB penetration that may hamper the further development of 2-aminoimidazoles endowed with *in vitro* low nanomolar profiles [29].

6. Conclusion

In this paper, we have described a rational structure-based approach, integrated with a synthetic protocol amenable to parallel synthesis, aimed at the discovery of new 2-aminoimidazole derivatives as BACE-1 inhibitors. Among 10 novel derivatives, **7** has emerged as a promising anti-BACE-1 *hit* compound thanks to: i) a rather good chemical accessibility that allows to carry out extensive SAR studies; ii) a low micromolar inhibitory profile against BACE-1, as assessed by enzymatic and cellular assays; iii) the capability to cross *in vitro* the BBB. In conclusions, **7** can represent the starting point for an extensive campaign of *hit*-to-*lead* and eventually *lead* optimization.

7. Experimental section

7.1. General chemical methods

Reaction progress was monitored by TLC on precoated silica gel plates (Kieselgel 60 F254, Merck) and visualized by UV254 light. Flash column chromatography was performed on silica gel (particle size 40–63 μM, Merck). Tetrahydrofuran (THF) and Et_2O were freshly distilled over sodium/benzoketal. Unless otherwise stated, all reagents were obtained from commercial sources and used without further purification. Compounds **16**, **17** were obtained following a standard procedure as described in SI. Compounds were named relying on the naming algorithm developed by CambridgeSoft Corporation and used in Chem-BioDraw Ultra 11.0. ^1H NMR and ^{13}C NMR spectra were recorded at 200–400 and 50–100 MHz, respectively. All the NMR experiments were performed by using $CDCl_3$ as solvent. Chemical shifts (δ) are reported in parts per millions (ppm) relative to TMS as internal standard. Coupling constants (J), when given, are reported in Hertz (Hz). For microwave-assisted organic synthesis a CEM Discover BenchMate reactor was used in the standard configuration as delivered, including proprietary software. All microwave-assisted reactions were carried out in sealed quartz process vials (15 mL). IR-FT spectra were performed in Nujol and obtained on a Nicolet Avatar 320 E.S.P. instrument; ν_{max} is expressed in cm^{-1}. Mass spectra were recorded on a V.G. 7070 E spectrometer or on a Waters ZQ 4000 apparatus operating in electrospray (ES) mode. Purity of compounds was determined by elemental analyses; purity for all the tested compounds was ≥95%.

Table 1
BACE-1 inhibition profile of compounds **2**–**11**.

Cpds	Chemical structure	BACE-1 inhibition (%)[a,b]	BACE-1 IC_{50} (μM)[a]
2	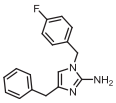	26.40 ± 0.02	n.d.[c]
3	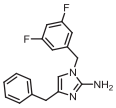	20.27 ± 0.01	n.d.
4	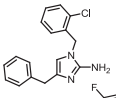	23.31 ± 0.01	n.d.
5	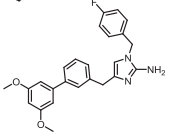	32.51 ± 0.01	n.d.
6	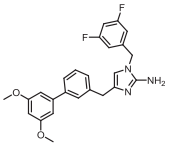	32.48 ± 0.01	n.d.
7	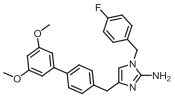	40.25 ± 0.01	7.40 ± 1.20
8	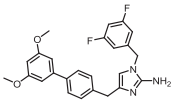	38.17 ± 0.05	7.32 ± 0.54
9	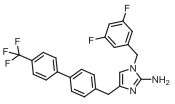	41.34 ± 0.01	5.59 ± 0.06
10	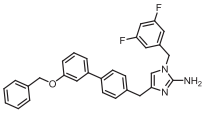	24.25 ± 0.02	n.d.
11	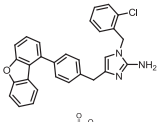	37.78 ± 0.01	5.95 ± 0.17
IV[d]	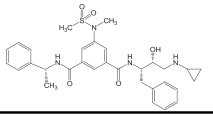	>80	0.01 ± 0.00

[a] Values are mean ± S.D. of two independent experiments for BACE-1 inhibition [20].
[b] % inhibition of BACE-1 activity at the concentration of 5 μM of the tested compounds **2**–**11**.
[c] n.d. = not determined.
[d] Reference BACE-1 inhibitor, β-secretase inhibitor IV, Calbiochem, UK.

7.2. General procedure for the microwave-assisted synthesis of 2-aminoimidazoles, *1*–*11*

In a 10 mL microwave vial, 2-benzylaminopyrimidines **12a**–**d** (1.0 equiv) and 3-substituted-α-bromopropyl aldehydes **13a**–**f** (1.35 equiv) were successively dissolved in dry CH_3CN (2–3 mL). The microwave reactor was irradiated by maximum power of 150 W at the temperature of 150 °C for 75 min. After the reaction mixture was cooled with an air flow for 15 min, a hydrazine hydrate 60% solution (5 equiv) was added, and the mixture was irradiated at 100 W to heat at the temperature of 100 °C for 15 min. The reaction mixture was diluted by CH_2Cl_2 (20 mL), washed with a saturated NH_4Cl solution (10 mL), brine (10 mL) and H_2O (2 × 10 mL). The organic layer was dried over Na_2SO_4, then filtered and concentrated. The resulting residue was purified by flash chromatography on silica gel (CH_2Cl_2/MeOH = 9.5/0.5) (Scheme 1).

7.2.1. 4-Benzyl-1-(4-fluorobenzyl)-1H-imidazol-2-amine *2*

Reaction of *N*-(4-fluorobenzyl)pyrimidin-2-amine **12b** (0.25 g, 1.25 mmol) and 2-bromo-3-phenylpropanal **13f** (0.36 g, 1.68 mmol) gave the crude final product **2** that was purified by flash chromatography (CH_2Cl_2/MeOH = 9.5/0.5). Yield 29%; brown semisolid; ESI-MS (*m*/*z*): 282 ($M + H^+$); ^{1}H NMR (200 MHz): δ 7.28–7.12 (m, 7H), 7.05–6.96 (m, 2H), 6.04 (s, 1H), 5.94 (br-s, 2H, NH_2), 4.87 (s, 2H), 3.73 (s, 2H) ppm; ^{13}C NMR (50 MHz): δ 164.7, 159.8, 147.4, 138.3, 131.0, 130.9, 129.2, 129.1, 128.7, 128.3, 126.3, 116.0, 115.5, 111.5, 47.8, 33.0 ppm. IR: $\nu = 3422\ cm^{-1}$.

7.2.2. 4-Benzyl-1-(3,5-difluorobenzyl)-1H-imidazol-2-amine *3*

Reaction of *N*-(3,5-difluorobenzyl)pyrimidin-2-amine **12c** (0.27 g, 1.25 mmol) and 2-bromo-3-phenylpropanal **13f** (0.36 g, 1.68 mmol) gave the crude final product **3** that was purified by flash chromatography (CH_2Cl_2/MeOH = 9.5/0.5). Yield 21%; brown semisolid; ESI-MS (*m*/*z*): 300 ($M + H^+$); ^{1}H NMR (200 MHz): δ 7.29–7.20 (m, 5H), 6.71–6.67 (m, 3H), 6.10 (s, 1H), 5.10 (br-s, 2H, NH_2), 4.89 (s, 2H), 3.77 (s, 2H) ppm; ^{13}C NMR (50 MHz): δ 165.8 (d, $J = 12.5$), 160.8 (d, $J = 12.5$), 148.2, 139.0, 138.7, 137.7, 132.2, 128.8, 128.5, 126.6, 111.2, 110.0, 103.8 (t, $J = 25$), 47.6, 32.6 ppm. IR: $\nu = 3421\ cm^{-1}$.

7.2.3. 4-Benzyl-1-(2-chlorobenzyl)-1H-imidazol-2-amine *4*

Reaction of *N*-(2-chlorobenzyl)pyrimidin-2-amine **12d** (0.27 g, 1.25 mmol) and 2-bromo-3-phenylpropanal **13f** (0.36 g, 1.68 mmol) gave the crude final product **4** that was purified by flash chromatography (CH_2Cl_2/MeOH = 9.5/0.5). Yield 11%; brown semisolid; ESI-MS (*m*/*z*): 299 ($M + H^+$); ^{1}H NMR (200 MHz): δ 7.40–7.23 (m, 8H), 7.07–7.02 (m, 1H), 5.96 (s, 1H), 4.95 (s, 2H), 4.80 (br-s, 2H, NH_2) 3.80 (s, 2H) ppm; ^{13}C NMR (50 MHz): δ 148.1, 137.8, 133.0, 132.3, 131.5, 129.9, 129.8, 128.9, 128.7, 128.5, 127.5, 126.6, 111.3, 46.2, 32.5 ppm. IR: $\nu = 3420\ cm^{-1}$.

7.2.4. 1-(4-Fluorobenzyl)-4-((3′,5′-dimethoxybiphenyl-3-yl) methyl)-1H-imidazol-2-amine *5*

Reaction of *N*-(4-fluorobenzyl)pyrimidin-2-amine **12b** (0.25 g, 1.25 mmol) and 2-bromo-3-(3′,5′-dimethoxybiphenyl-3-yl)propanal **13a** (0.58 g, 1.68 mmol) gave the crude final product **5** that was purified by flash chromatography (CH_2Cl_2/MeOH = 9.5/0.5). Yield 21%; orange solid; m.p. 76.5–80.0 °C decomposed; ESI-MS (*m*/*z*): 418 ($M + H^+$); ^{1}H NMR (200 MHz): δ 7.48–7.25 (m, 4H), 7.15–6.99 (m, 4H), 6.74–6.73 (m, 2H), 6.48–6.46 (m, 1H), 6.21 (s, 1H), 4.79 (s, 2H), 3.99 (br-s, 2H, NH_2), 3.85 (s, 6H), 3.82 (s, 2H) ppm; ^{13}C NMR (50 MHz): δ 164.8, 161.0, 159.9, 147.5, 143.5, 141.1, 140.4, 136.7, 131.8, 131.7, 128.7, 128.5, 128.1, 127.7, 124.9, 116.1, 115.7, 112.4, 105.5, 99.1, 55.4, 47.8, 34.8 ppm. IR: $\nu = 3414\ cm^{-1}$.

7.2.5. 1-(3,5-Difluorobenzyl)-4-((3′,5′-dimethoxybiphenyl-3-yl) methyl)-1H-imidazol-2-amine *6*

Reaction of *N*-(3,5-difluorobenzyl)pyrimidin-2-amine **12c** (0.27 g, 1.25 mmol) and 2-bromo-3-(3′,5′-dimethoxybiphenyl-3-yl) propanal **13a** (0.58 g, 1.68 mmol) gave the crude final product **6** that was purified by flash chromatography (CH_2Cl_2/MeOH = 9.5/0.5). Yield 22%; brown semisolid; ESI-MS (*m*/*z*): 436 ($M + H^+$); ^{1}H NMR

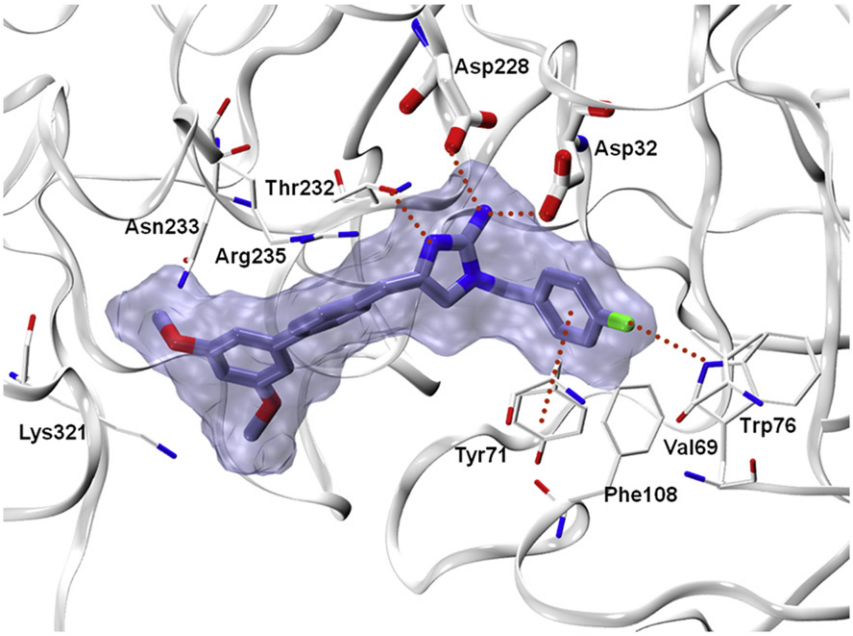

Fig. 2. The binding mode of **7** at the proteasic domain of BACE-1 (PDB ID: 1SGZ) [23] with the key interactions shown by orange points. (For interpretation of the references to colour in this figure legend, the reader is referred to the web version of this article.)

(400 MHz): δ 7.46–7.44 (m, 1H), 7.42–7.40 (m, 1H), 7.35–7.31 (m, 1H), 7.24–7.21 (m, 2H), 6.75–6.70 (m, 2H), 6.69–6.61 (m, 2H), 6.44–6.43 (m, 1H), 6.04 (s, 1H), 4.79 (s, 2H), 4.82 (s, 6H), 3.80 (s, 2H), 2.78 (br-s, 2H, NH_2) ppm; ^{13}C NMR (50 MHz): δ 165.7 (d, $J = 12.5$), 161.7 (d, $J = 12.5$), 148.0, 143.3, 141.0, 140.3, 140.2, 136.9, 128.6, 128.1, 127.7, 124.9, 112.0, 109.8, 109.6, 109.3, 105.4, 103.3 (t, $J = 25$), 99.2, 55.3, 47.4, 34.7 ppm. IR: $\nu = 3415$ cm^{-1}.

7.2.6. 1-(4-Fluorobenzyl)-4-((3′,5′-dimethoxybiphenyl-4-yl) methyl)-1H-imidazol-2-amine **7**

Reaction of *N*-(4-fluorobenzyl)pyrimidin-2-amine **12b** (0.25 g, 1.25 mmol) and 2-bromo-3-(3′,5′-dimethoxybiphenyl-4-yl)propanal **13b** (0.58 g, 1.68 mmol) gave the crude final product **7** that was purified by flash chromatography (CH_2Cl_2/MeOH = 9.5/0.5). Yield 30%; yellow solid; m.p. 156.5–161.2 °C decomposed; ESI-MS (*m*/*z*): 418 ($M + H^+$); ^1H NMR (400 MHz): δ 7.47 (d, $J = 8.4$, 2H), 7.31 (d, $J = 8.4$, 2H), 7.10–7.08 (m, 2H), 7.04–6.99 (m, 2H), 6.70–6.69 (m, 2H), 6.44–6.43 (m, 1H), 6.02 (s, 1H), 4.79 (s, 2H), 3.82 (s, 6H), 3.79 (s, 2H), 1.96 (br-s, 2H, NH_2) ppm; ^{13}C NMR (50 MHz) δ 164.0, 161.0, 159.0, 147.4, 143.3, 139.3, 139.0, 136.6, 131.7, 129.2, 128.7, 128.5, 127.1, 116.2, 115.8, 112.4, 105.3, 99.1, 55.4, 47.9, 34.3 ppm. IR: $\nu = 3414$ cm^{-1}.

7.2.7. 1-(3,5-Difluorobenzyl)-4-((3′,5′-dimethoxybiphenyl-4-yl) methyl)-1H-imidazol-2-amine ***8***

Reaction of *N*-(3,5-difluorobenzyl)pyrimidin-2-amine **12c** (0.28 g, 1.25 mmol) and 2-bromo-3-(3′,5′-dimethoxybiphenyl-4-yl) propanal **13b** (0.59 g, 1.69 mmol) gave the crude final product **8** that was purified by flash chromatography (CH_2Cl_2/MeOH = 9.5/0.5). Yield 31%; yellow solid; m.p. 142.5–145.5 °C decomposed; ESI-MS (*m*/*z*): 436 ($M + H^+$); ^1H NMR (400 MHz): δ 7.49 (d, $J = 8.4$, 2H), 7.32 (d, $J = 8.4$, 2H), 6.73–6.70 (m, 1H), 6.69–6.68 (m, 2H), 6.65–6.62 (m, 2H), 6.43–6.42 (m, 1H), 6.21 (s, 1H), 4.81 (s, 2H), 3.83 (s, 2H), 3.82 (s, 6H), 1.64 (br-s, 2H, NH_2) ppm; ^{13}C NMR (50 MHz) δ 165.8 (d, $J = 12.5$), 161.0 (d, $J = 12.5$), 147.7, 143.2, 140.4, 140.2, 140.1, 139.4, 138.9, 137.2, 129.2, 127.1, 112.2, 109.8, 109.3, 105.2, 103.4 (t, $J = 25$), 99.0, 55.3, 47.6, 34.3 ppm. IR: $\nu = 3415$ cm^{-1}.

7.2.8. 1-(3,5-Difluorobenzyl)-4-((4′-(trifluoromethyl)biphenyl-4-yl) methyl)-1H-imidazol-2-amine ***9***

Reaction of *N*-(3,5-difluorobenzyl)pyrimidin-2-amine **12c** (0.15 g, 0.70 mmol) and 2-bromo-3-(4′-(trifluoromethyl)biphenyl-4-yl)propanal **13c** (0.34 g, 0.95 mmol) gave the crude final product **9** that was purified by flash chromatography. Yield 26%; yellow solid; m.p. 164.0–169.0 °C decomposed; ESI-MS (*m*/*z*): 444

Table 2
Inhibition of $A\beta_{38}$, $A\beta_{40}$ and $A\beta_{42}$ secretion,[a] *in vitro* permeability (*Pe*) values[b] with related predictive penetration into the CNS[c] and molecular descriptors[d] of compounds **7**–**9** and **11**.

Cpds	$A\beta_{38}$ IC_{50} (μM)[a]	$A\beta_{40}$ IC_{50} (μM)[a]	$A\beta_{42}$ IC_{50} (μM)[a]	*Pe* (10^{-6} cm s^{-1})[b]	Prediction[c]	cLogP (prot.)[d]	cLogP (not prot.)[d]	TPSA (prot.)[d]	TPSA (not prot.)[d]
7	15	23	19	4.0 ± 1.0	CNS+	2.572	5.593	63.562	62.317
8	33	35	27	3.2 ± 0.2	CNS+/−	2.663	5.685	63.562	62.317
9	n.a.[e]	n.a.	n.a.	n.d.[f]	n.d.	3.517	6.539	45.094	43.849
11	n.a.	n.a.	n.a.	4.0 ± 0.7	CNS+	4.581	7.602	58.234	56.989

[a] Values are mean of three independent experiments for reduction of Aβ secretion. All data were corrected with mean neurons viability obtained in the MTT reduction assay, performed after 24 h of treatment with these BACE-1 inhibitors to evaluate their potential cell toxicity.
[b] Values are mean ± S.D. of two independent experiments (PBS/EtOH = 70/30 was used as solvent).
[c] The compounds were classified [26] as CNS+ when they present a *Pe* value >3.55 × 10^{-6} cm s^{-1}, and as CNS+/− when the *Pe* value is between 3.55 × 10^{-6} and 2.00 × 10^{-6} cm s^{-1}.
[d] cLogP and TPSA in both protonated and not protonated were calculated by Molinspiration, a free-online cheminformatics tool (http://www.molinspiration.com).
[e] n.a. = not active.
[f] n.d. = not determined.

($M + H^+$); ^{1}H NMR (400 MHz): δ 7.66–7.64 (m, 4H), 7.53 (d, $J = 8.4$, 2H), 7.36 (d, $J = 8.4$, 2H), 6.76–6.75 (m, 1H), 6.66–6.65 (m, 2H), 6.08 (s, 1H), 4.81 (s, 2H), 3.83 (s, 2H), 3.06 (br-s, 2H, NH_2) ppm; ^{13}C NMR (100 MHz): δ 164.6 (d, $J = 12.3$), 162.1 (d, $J = 12.3$), 148.3, 144.3, 138.5, 138.1, 137.9, 132.1, 129.5, 129.1, 127.5, 127.2, 125.7, 125.6, 122.1, 111.2, 110.1, 109.9, 104.0 (t, $J = 24.6$), 47.6, 32.2 ppm. IR: $\nu = 3418$ cm^{-1}.

7.2.9. 1-(3,5-Difluorobenzyl)-4-((3′-(benzyloxy)biphenyl-4-yl) methyl)-1H-imidazol-2-amine **10**

Reaction of *N*-(3,5-difluorobenzyl)pyrimidin-2-amine **12c** (0.18 g, 0.82 mmol) and 2-bromo-3-(3′-(benzyloxy)biphenyl-4-yl) propanal **13d** (0.44 g, 1.11 mmol) gave the crude final product **10** that was purified by flash chromatography (CH_2Cl_2/MeOH = 9.5/0.5). Yield 23%; yellow solid; m.p. 166.0–171.0 °C decomposed; ESI-MS (*m*/*z*): 482 ($M + H^+$); ^{1}H NMR (200 MHz): δ 7.56–7.29 (m, 10H), 7.21–7.18 (m, 2H), 6.99–6.96 (m, 1H), 6.82–6.98 (m, 3H), 6.01 (s, 1H), 5.14 (s, 2H), 4.88 (s, 2H), 3.84 (s, 2H), 2.02 (br-s, 2H, NH_2) ppm; ^{13}C NMR (50 MHz): δ 160.8 (d, $J = 12.5$), 159.1 (d, $J = 12.5$), 147.3, 142.6, 139.2, 138.8, 137.6, 137.0, 130.9, 129.7, 129.3, 128.6, 128.0, 127.5, 127.2, 119.8; 113.7, 113.3, 112.6, 109.9, 109.4, 103.6 (t, $J = 25$), 70.1, 47.7, 34.5 ppm. IR: $\nu = 3415$ cm^{-1}.

7.2.10. 1-(2-Chlorobenzyl)-4-(4-(dibenzo[b,d]furan-1-yl)benzyl)-1H-imidazol-2-amine **11**

Reaction of *N*-(2-chlorobenzyl)pyrimidin-2-amine **12d** (0.15 g, 0.68 mmol) and 2-bromo-3-(4-(dibenzo[*b*,*d*]furan-1-yl)phenyl) propanal **13e** (0.35 g, 0.92 mmol) gave the crude final product **11** that was purified by flash chromatography (CH_2Cl_2/MeOH = 9.5/0.5). Yield 13%; yellow solid; m.p. 76.2–81.2 °C decomposed; ESI-MS (*m*/*z*): 465 ($M + H^+$); ^{1}H NMR (400 MHz): δ 7.97–7.95 (m, 1H), 7.91–7.88 (m, 1H), 7.83–7.81 (m, 2H), 7.58–7.55 (m, 2H), 7.46–7.31 (m, 6H), 7.25–7.22 (m, 2H), 6.94–6.92 (m, 1H), 6.25 (s, 1H), 4.92 (s, 2H), 3.87 (s, 2H), 2.63 (br-s, 2H, NH_2) ppm; ^{13}C NMR (100 MHz): δ 156.1, 153.3, 148.2, 136.9, 135.0, 133.1, 131.8, 130.3, 130.0, 129.9, 129.1, 129.0, 128.8, 127.6, 127.2, 126.7, 125.4, 124.9, 124.1, 123.2, 122.8, 120.6, 119.6, 111.8, 111.3, 46.4, 31.8 ppm. IR: $\nu = 3413$ cm^{-1}.

7.3. General parallel procedure for the synthesis of 2-benzylaminopyrimidines **12a–d**

In distinct reactors, 2-aminopyrimidine **15** (4 equiv) was dissolved in dry THF (12 mL) and the resulting solution was cooled in an ice bath. To these solutions NaH (4 equiv) was added resulting in effervescence and in the formation of suspensions. The mixtures were stirred in the ice bath for 15 min, and then the appropriate benzyl bromide derivates **14a–d** (1 equiv) were added dropwise to each reactor. The mixtures were stirred at room temperature for 24 h and each one was treated as follow. The solvent was evaporated under vacuo, and H_2O (25 mL) was added. The resulting aqueous solution was extracted with CH_2Cl_2 (3 × 25 mL) and the combined organic layers were washed with H_2O (25 mL), saturated $NaHCO_3$ solution (25 mL) and brine (25 mL), dried over anhydrous Na_2SO_4 and concentrated under vacuo. Each crude residue was purified by flash chromatography on silica gel (petroleum ether/EtOAc = 1/1) (Scheme 2).

7.3.1. N-(4-fluorobenzyl)pyrimidin-2-amine **12b**

Reaction of 2-aminopyrimidine **15** (1.5 g, 15.75 mmol) and the benzyl bromide **14b** (0.49 mL, 3.96 mmol) afforded compound **12b** that was purified on silica gel (petroleum ether/EtOAc = 1/1). Yield 83%; white solid; m.p. 89.5–90.5 °C; ^{1}H NMR (200 MHz): δ 8.29 (d, $J = 4.6$, 2H), 7.38–7.29 (m, 2H), 7.08–6.99 (m, 2H), 6.58 (t, $J = 4.8$, 1H), 5.62 (br-s, 1H, NH), 4.63 (d, $J = 6.0$, 2H) ppm.

7.4. General parallel procedure for the synthesis of biphenyl propanoic acid methyl esters **22a–e**

In distinct reactors, 3-(bromophenyl)-propionic methyl esters **16**, **17** (1.0 equiv) were dissolved in toluene (7 mL). Phenyl boronic acids **18–21** (2 equiv) in EtOH (3.5 mL) and Na_2CO_3 2 M (2 M, aq, 3.0 equiv) were then added to the corresponding reactors, and the resulting mixtures were deoxygenated with a stream of N_2. After 10 min, $Pd(PPh_3)_4$ (0.005 equiv) was added and each mixture was stirred at reflux temperature for 5 h under N_2, then cooled to room temperature and treated as follows. Each solution was poured into a mixture of H_2O (5 mL) and Et_2O (5 mL), and the two phases were separated. The aqueous layer was washed with Et_2O (5 mL), and the organic phases were combined and washed with 1 M NaOH (5 mL), followed by brine (5 mL), then dried over Na_2SO_4 and evaporated. Purification of each crude product performed by flash chromatography on silica gel (petroleum ether/EtOAc = 8/2) yielded the corresponding biphenyl propanoic acid methyl esters **22a–e** (Scheme 3).

7.4.1. Methyl 3-(3′,5′-dimethoxybiphenyl-4-yl)propanoate **22b**

Reaction of 3-(bromophenyl)-propionic methyl ester **17** (0.3 g, 1.23 mmol) and boronic acid **18** (0.45 g, 2.46 mmol) afforded compound **22b** that was purified by flash chromatography on silica gel (petroleum ether/EtOAc = 8/2). Yield 94%; white powder; m.p. 50.0–52.0 °C; ^{1}H NMR (200 MHz): δ 7.52 (d, $J = 7.8$, 2H), 7.29 (d, $J = 8.0$, 2H), 6.75–6.74 (m, 2H), 6.49–6.48 (m, 1H), 3.87 (s, 6H), 3.71 (s, 3H), 3.02 (t, $J = 7.6$, 2H), 2.69 (t, $J = 7.6$, 2H) ppm.

7.5. General procedure for the synthesis of 3-biphenyl propyl alcohols **23a–e**

$LiAlH_4$ (1.2 equiv) was dissolved in dry Et_2O (2 mL) and to the resulting suspension cooled at 0 °C a solution of the appropriate biphenyl propanoic methyl esters **22a–e** (1.0 equiv) in dry Et_2O was added dropwise. The reaction mixture was stirred at room temperature for 5 h under N_2 atmosphere. The mixture was cooled to 0 °C and quenched with sequential additions of H_2O (1 mL), NaOH 10% (0.8 mL) and H_2O (1 mL). The aqueous suspension was extracted with Et_2O (3 × 10 mL). The combined organic layers were dried over Na_2SO_4 and evaporated to dryness. The crude products were used in a further reaction without purification (Scheme 3).

7.5.1. 3-(3′,5′-Dimethoxybiphenyl-4-yl)propan-1-ol **23b**

Biphenyl propanoic methyl ester **22b** (0.15 g, 0.50 mmol) led to compound **23b**. Yield 99%; white powder; m.p. 80.5–81.5 °C; ^{1}H NMR (200 MHz): δ 7.40 (d, $J = 8.2$, 2H), 7.14 (d, $J = 7.8$, 2H), 6.63–6.62 (m, 2H), 6.36–6.34 (m, 1H), 3.73 (s, 6H), 3.58 (t, $J = 6.6$, 2H), 2.64 (t, $J = 7.2$, 2H), 1.88–1.74 (m, 2H), 1.82 (br-s, 1H, OH) ppm.

7.6. General procedure for the synthesis of 3-susbstituted propyl aldehydes **24a–f**

A solution of the appropriate 3-biphenyl propyl alcohols **23a–f** (1.0 equiv) in CH_2Cl_2 (5 mL) was added dropwise to the suspension of PCC (1.4 equiv) in CH_2Cl_2 (15 mL) cooled to 0 °C. The reaction mixture was stirred in an ice bath for 3–4 h, then filtered on silica gel and evaporated to dryness. All the compounds were used in the next step without any further purification (Scheme 3).

7.6.1. 3-(3′,5′-Dimethoxybiphenyl-4-yl)propanal **24b**

3-Biphenyl propyl alcohol **23b** (0.42 g, 1.54 mmol) lead to compound **24b**. Yield 72%; yellow oil; ^{1}H NMR (400 MHz): δ 9.82 (t, $J = 1.2$, 1H), 7.50 (d, $J = 6.8$, 2H), 7.24 (d, $J = 7.6$, 2H), 6.72–6.71 (m, 2H), 6.47–6.45 (m, 1H), 3.83 (s, 6H), 2.98 (t, $J = 7.6$, 2H), 2.79 (t, $J = 7.2$, 2H) ppm.

7.7. General procedure for the synthesis of 3-susbstituted-α-bromopropyl aldehydes **13a–f**

A solution of the appropriate 3-susbstituted propyl aldehydes **24a–f** (1.0 equiv) in dry Et_2O (2 mL) was added dropwise to a solution of DBBA (0.5 equiv) in dry Et_2O (4 mL). Successively, a solution 4 N of HCl in 1,4-dioxane (0.028 mL, 0.1 equiv) was added dropwise and the reaction mixture was stirred at room temperature for 20 h. The resulting suspension was extracted with a saturated $NaHCO_3$ solution (10 mL) and Et_2O (3×10 mL). The combined organic layers were washed with H_2O (10 mL), and brine (10 mL), then dried over Na_2SO_4 and evaporated to dryness (Scheme 3).

7.7.1. 2-Bromo-3-(3′,5′-dimethoxybiphenyl-4-yl)propanal **13b**

3-susbstituted propyl aldehyde **24b** (0.47 g, 1.73 mmol) led to the brominated product **13b**. Yield 99%; thick yellow oil; ^{1}H NMR (200 MHz): δ 9.55 (d, $J = 1.8$, 1H), 7.57–7.54 (m, 1H), 7.40–7.28 (m, 3H), 6.74–6.73 (m, 1H), 6.53–6.49 (m, 2H), 4.57–4.46 (m, 1H), 3.87 (s, 6H), 3.62–3.45 (m, 2H) ppm.

7.8. Molecular docking

The model of BACE-1 was constructed by removing all water molecules from the X-ray structure of human BACE-1 “apo” form (PDB ID: 1SGZ). Hydrogen atoms were added and minimized by Amber force field Parm99 [30]. Histidines were protonated according to their putative H-bond patterns in the crystal structure. The 3D models of ligands were built using Sybyl 7.1.1 (Tripos Associates Inc, USA) and then optimized at the density functional level of theory (B3LYP/6-31G*) by means of the Gaussian 09 [31] software. Docking simulations were carried out by means of GOLD [32], 4.1.1 version (see SI). The outcomes from docking were clusterized by using AClAP [33,34].

Acknowledgments

The authors acknowledge the Italian Institute of Technology (IIT) and the University of Bologna for the financial support. G.C. thanks Dr. M. Masetti for valuable scientific discussions, and Ms S. Leone and Ms R. Manfroni for their technical assistance. M.L.B. thanks Dr. S. Czvitkovich and Dr. M. Windisch from JSW for their scientific contribution. D.I.P. acknowledges a postdoctoral fellowship from the CSIC (JAE program). Thanks are due to CIRB (University of Bologna) for the use of Fluoroskan Ascent multiwell spectrofluorometer and to Prof. D. Simoni (University of Ferrara) for the use of CEM Discover BenchMate reactor.

Appendix. Supplementary information

Supplementary Information associated with this article can be found, in the online version, at doi:10.1016/j.ejmech.2011.12.016.

References

[1] D.J. Selkoe, Nature 399 (1999) A23–A31.
[2] C. Haass, D.J. Selkoe, Nat. Rev. Mol. Cell. Biol. 8 (2007) 101–112.
[3] M. Citron, Nat. Rev. Drug Discov. 9 (2010) 387–398.
[4] M. Bartolini, V. Andrisano, ChemBioChem 11 (2010) 1018–1035.
[5] M.L. Bolognesi, R. Matera, A. Minarini, M. Rosini, C. Melchiorre, Curr. Opin. Chem. Biol. 13 (2009) 303–308.
[6] F. Panza, V. Solfrizzi, V. Frisardi, C. Capurso, A. D'Introno, A.M. Colacicco, G. Vendemiale, A. Capurso, B.P. Imbimbo, Drugs Aging 26 (2009) 537–555.
[7] R.J. Kelleher, J. Shen, Science 330 (2010) 1055–1056.
[8] M.K. Holloway, P. Hunt, G.B. McGaughey, Drug Dev. Res. 70 (2009) 70–93.
[9] L. Hong, G. Koelsch, X. Lin, S. Wu, S. Terzyan, A.K. Ghosh, X.C. Zhang, J. Tang, Science 290 (2000) 150–153.
[10] L. Hong, R.T. Turner, G. Koelsch, D. Shin, A.K. Ghosh, J. Tang, Biochemistry 41 (2002) 10963–10967.
[11] Huang Wen-Hai, Sheng Rong, H. Yong-Zhou, Curr. Med. Chem. 16 (2009) 1806–1820.
[12] R. Silvestri, Med. Res. Rev. 29 (2009) 295–338.
[13] X. Luo, R. Yan, Int. J. Clin. Exp. Pathol. 3 (2010) 618–628.
[14] G. Chiriano, A. Sartini, F. Mancini, V. Andrisano, M.L. Bolognesi, M. Roberti, M. Recanatini, P. Carloni, A. Cavalli, Chem. Biol. Drug Des. 77 (2011) 268–271.
[15] M. Haniu, P. Denis, Y. Young, E.A. Mendiaz, J. Fuller, J.O. Hui, B.D. Bennett, S. Kahn, S. Ross, T. Burgess, V. Katta, G. Rogers, R. Vassar, M. Citron, J. Biol. Chem. 275 (2000) 21099–21106.
[16] J.D. Sullivan, R.L. Giles, R.E. Looper, Curr. Bioact. Compd. 5 (2009) 39–78.
[17] D.S. Ermolat'ev, J.B. Bariwal, H.P.L. Steenackers, S.C.J. De Keersmaecker, E.V. Van der Eycken, Angew. Chem. Int. Ed. Engl. 49 (2010) 9465–9468.
[18] D.S. Ermolat'ev, E.V. Babaev, E.V. Van der Eycken, Org. Lett. 8 (2006) 5781–5784.
[19] H.P. Steenackers, D.S. Ermolat'ev, B. Savaliya, A.D. Weerdt, D.D. Coster, A. Shah, E.V. Van der Eycken, D.E. De Vos, J. Vanderleyden, S.C. De Keersmaecker, J. Med. Chem. 54 (2011) 472–484.
[20] P. Camps, X. Formosa, C. Galdeano, D. Muñoz-Torrero, L. Ramírez, E. Gómez, N. Isambert, R. Lavilla, A. Badia, M.V. Clos, M. Bartolini, F. Mancini, V. Andrisano, M.P. Arce, M.I. Rodríguez-Franco, Ó Huertas, T. Dafni, F.J. Luque, J. Med. Chem. 52 (2009) 5365–5379.
[21] S. Czvitkovich, S. Duller, E. Mathiesen, K. Lorenzoni, B. Imbimbo, B. Hutter-Paier, M. Windisch, R. Wronski, J. Mol. Neurosci. 43 (2010) 257–267.
[22] W.K. Hagmann, J. Med. Chem. 51 (2008) 4359–4369.
[23] L. Hong, J. Tang, Biochemistry 43 (2004) 4689–4695.
[24] S.J. Stachel, C.A. Coburn, D. Rush, K.L.G. Jones, H. Zhu, H. Rajapakse, S.L. Graham, A. Simon, M. Katharine Holloway, T.J. Allison, S.K. Munshi, A.S. Espeseth, P. Zuck, D. Colussi, A. Wolfe, B.L. Pietrak, M.-T. Lai, J.P. Vacca, Bioorg. Med. Chem. Lett. 19 (2009) 2977–2980.
[25] I.D. Hills, M.K. Holloway, P. de León, A. Nomland, H. Zhu, H. Rajapakse, T.J. Allison, S.K. Munshi, D. Colussi, B.L. Pietrak, D. Toolan, S.J. Haugabook, S.L. Graham, S.J. Stachel, Bioorg. Med. Chem. Lett. 19 (2009) 4993–4995.
[26] L. Di, E.H. Kerns, K. Fan, O.J. McConnell, G.T. Carter, Eur. J. Med. Chem. 38 (2003) 223–232.
[27] L.K. Chico, L.J. Van Eldik, D.M. Watterson, Nat. Rev. Drug Discov. 8 (2009) 892–909.
[28] W.M. Pardridge, Alzheimers Dement. 5 (2009) 427–432.
[29] M.S. Malamas, J. Erdei, I. Gunawan, K. Barnes, M. Johnson, Y. Hui, J. Turner, Y. Hu, E. Wagner, K. Fan, A. Olland, J. Bard, A.J. Robichaud, J. Med. Chem. 52 (2009) 6314–6323.
[30] J. Wang, P. Cieplak, P.A. Kollman, J. Comput. Chem. 21 (2000) 1049–1074.
[31] M.J. Frisch, G.W. Trucks, H.B. Schlegel, G.E. Scuseria, M.A. Robb, J.R. Cheeseman, G. Scalmani, V. Barone, B. Mennucci, G.A. Petersson, H. Nakatsuji, M. Caricato, X. Li, H.P. Hratchian, A.F. Izmaylov, J. Bloino, G. Zheng, J.L. Sonnenberg, M. Hada, M. Ehara, K. Toyota, R. Fukuda, J. Hasegawa, M. Ishida, T. Nakajima, Y. Honda, O. Kitao, H. Nakai, T. Vreven, J.A. Montgomery Jr., J.E. Peralta, F. Ogliaro, M. Bearpark, J.J. Heyd, E., Brothers, K.N. Kudin, V.N. Staroverov, R. Kobayashi, J. Normand, K. Raghavachari, A. Rendell, J.C. Burant, S.S. Iyengar, J. Tomasi, M. Cossi, N. Rega, N.J. Millam, M. Klene, J.E. Knox, J.B. Cross, V. Bakken, C. Adamo, J. Jaramillo, R. Gomperts, R.E. Stratmann, O. Yazyev, A.J. Austin, R. Cammi, C. Pomelli, J.W. Ochterski, R.L. Martin, K. Morokuma, V.G. Zakrzewski, G.A. Voth, P. Salvador, J.J. Dannenberg, S. Dapprich, A.D. Daniels, Ö. Farkas, J.B. Foresman, J.V. Ortiz, J. Cioslowski, D.J. Fox, Gaussian Inc., Wallingford CT, 2009.
[32] G. Jones, P. Willett, R.C. Glen, A.R. Leach, R. Taylor, J. Mol. Biol. 267 (1997) 727–748.
[33] G. Bottegoni, A. Cavalli, M. Recanatini, J. Chem. Inf. Model. 46 (2006) 852–862.
[34] G. Bottegoni, W. Rocchia, M. Recanatini, A. Cavalli, Bioinformatics 22 (2006) e58–e65.